Desalination and Water Treatment
www.deswater.com
doi: 10.1080/19443994.2015.1054312

57 (2016) 12496–12507
June

Taylor & Francis
Taylor & Francis Group

Photocatalytic activity of zinc oxide (ZnO) synthesized through different methods

NikAthirah Yusoff[a], Li-Ngee Ho[b,*], Soon-An Ong[a], Yee-Shian Wong[a], WanFadhilah Khalik[a]

[a]*Water Research Group (WAREG), School of Environmental Engineering, University Malaysia Perlis, Arau 02600, Perlis, Malaysia, emails: athirah_yusoff@ymail.com (N.A. Yusoff), ongsoonan@yahoo.com (S.-A. Ong), yswong@unimap.edu.my (Y.-S. Wong), wanfadhilah@ymail.com (W.F. Khalik)*
[b]*School of Materials Engineering, University Malaysia Perlis, Arau 02600, Perlis, Malaysia, Tel. +60 49768196; Fax: +60 49798178; email: holingee@yahoo.com*

Received 16 July 2014; Accepted 19 May 2015

ABSTRACT

Derivatives of phenol are considered as part of the persistent organic pollutants with endocrine effects persist in the environment and resist to bio-degradation which is difficult to be degraded. The objective of this study was to investigate the solar-photocatalytic degradation of phenol with synthesized ZnO through precipitation (ZnO-P) and hydrothermal (ZnO-H) method as photocatalysts. ZnO-P is capable to achieve total degradation of phenol up to 30 mg/l of initial phenol concentration and 20 mg/l for ZnO-H within 6 h of reaction time. The degradation of ZnO-P and ZnO-H is favored in acidic condition (pH 3) and followed by natural condition (pH 6). The results obtained fitted well with Langmuir–Hinshelwood kinetic model. The apparent rate constant is proportional to the efficiency of the photocatalysts. Chemical oxygen demand results attested the complete degradation of phenol concentration and possibility for mineralization.

Keywords: Zinc oxide; Precipitation; Hydrothermal; Photodegradation; Phenol

1. Introduction

Recent development in industries such as pesticides, pharmaceutical, petrochemicals, and oil refinery has led to a renewed interest in various wastewater treatment applications. However, far too little attention has been paid for the treatment of wastewater containing persistent organic pollutants with endocrine effects (POPs/EDCs). POPs are a synthetic organic chemicals either intentionally or non-intentionally produced [1]. Endocrine disruption is generally one of the important criteria in assessing risk and safe levels of POP. Some organic pollutant such as derivatives of phenolic compounds [2] considered as POPs/EDCs [3]. Assessment from McKinlay et al. [4] indicates that POPs/EDCs may be biologically active even at extremely low doses especially in ambient mixtures. Thus, the need of developing a suitable treatment method for the removal of POPs/EDCs has become one of the main interests of a quasi-consensus between researchers.

The physical removal through adsorption of powdered activated carbon (PAC) or granular activated carbon (GAC) was commonly utilized worldwide. However, Snyder et al. [5] reported its drawbacks,

*Corresponding author.

stated that the spent PAC and GAC must be disposed through land filling and it would produce another waste after treating another. Another option for POPs/EDCs treatment is through activated sludge biodegradation. The activated sludge process is mostly concentrated in large city's wastewater treatment and mainly to degrade organic compounds present in sewage treatment plants influent [6]. This type of treatment is very applicable for laboratory-scale experiments as several parameters need to be continuously controlled. Thus, it is a little bit unfeasible to be applied in conventional wastewater treatment. Furthermore, the pollutants adsorbed on activated sludge are potential to contaminate the soil and groundwater as the digested sludge has usually been applied as fertilizer in agriculture [6].

Recently, one of the advanced oxidation processes which is photocatalytic has gained a main attention due to its effectiveness of degrading the persistent or bio-resistant organic contaminant [7]. Fujishima et al. [8] reported the photocatalytic process occurred when photocatalyst reacted after the radiation energy that radiated on it, is higher than the band gap energy of the photocatalyst, thus producing hydroxyl radical (˙OH) to destroy the organic contaminant. Apparently photocatalyst played crucial roles in ensuring the success of photocatalytic treatment. Photocatalyst is defined as a semiconductor which activated through the photon absorption of radiation and consequently producing hydroxyl radical as oxidant to accelerate the reaction [9]. A well-known photocatalyst ZnO received much attention for photocatalytic application due to its effective, inexpensive, and non-toxic behavior [10]. It was decided that the best photocatalyst to adopt for this study was ZnO. Several factors are taken into account such as the high photosensitivity, stability, and large band gap [11] and high activity toward photocatalytic degradation of organic pollutant [12]. In this study also, the natural solar irradiation is used. Thus, the major advantage of ZnO is due to its adsorption over a larger fraction of the UV spectrum compared to other photocatalysts such as TiO_2 [13].

A wide variety of ZnO synthesis methods have been suggested, and basically it consists of three phases: the solid, the solution, and the vapor phase [14]. Overall, the metal oxide synthesis methods can be divided into liquid–solid and gas–solid transformations [15]. Liquid–solid transformation method was chosen for this research. The band gap of the synthesized ZnO was assumed as 3.2 eV as most value obtained by other researches which are 3.25 [16], 3.29, 3.21, 3.23 [17], and 3.19 eV [18]. In this paper, effect of synthesis method on the photodegradation of organic pollutant studied was phenol. The photocatalytic reaction was carried out by utilizing the ZnO photocatalyst synthesized through two different synthesis methods which were precipitation and hydrothermal methods. The characterization of each ZnO photocatalyst, effect of phenol concentration, pH, and mineralization of phenol were distinctively investigated. The kinetic study of the photodegradation of phenol was studied in order to evaluate the overall performances of the photocatalysts.

2. Experimental

2.1. Precipitation method

A total of 1.0 M zinc precursor $Zn(OAc)_2$ (Riedel-de Haen) was prepared with ultra-pure water and continuously stirred for 30 min at 60˚C. Then, 1.5 M of $NaHCO_3$ (HmbG Chemical) solution was added drop wise to $Zn(OAc)_2$ solution under vigorous stirring at 60˚C. The mixed solutions were allowed to mix for 2 h in 60˚C followed by cooling at room temperature and aging for overnight. The white precipitates formed were then filtered and rinsed several times with ultra-pure water and ethanol absolute (HmbG Chemical). The precipitates were then oven-dried for 6 h in 150˚C, ground and calcined at 350˚C for 1 h. The ZnO obtained from this precipitation method was denoted as ZnO-P.

2.2. Hydrothermal method

A total of 1.0 M $Zn(OAc)_2$ precursor solution was mixed with 1.5 M of $NaHCO_3$ solution in 60˚C for 2 h. Then, the mix solutions were transferred into Teflon-lined sealed stainless steel autoclave and heated to the temperature of 105˚C for 6 h under autogenous pressure. It was then allowed to cool at room temperature. The white precipitates were collected by filtration and rinsed with ultra-pure water and ethanol absolute. The precipitates were then oven-dried for 6 h in 150˚C to obtain ZnO precursor white powder. The powder ground and undergoes the calcination process at 350˚C for 1 h. The final white ZnO powdered from hydrothermal method was denoted ZnO-H.

2.3. Materials characterization

Scanning electron microscope (SEM) was utilized to analyze the morphology features of the photocatalyst. The SEM used to characterize the samples in this study was from JEOL, (Model: JSM-63O1F). The detailed information about the crystalline structure of the photocatalyst sample was measured on an X-ray

diffraction (XRD) from JEOL (Model: JDX-3530M), which used Cu-Kα radiation in the 2θ range of 10–100° at a scan speed of 5°/min.

2.4. Photocatalytic procedure

The photocatalytic of phenol crystallized 99% (detached crystal) (108-95-2) from Panreac was performed with 500 ml phenol solution being contacted with 0.6 g of synthesized photocatalyst ZnO. Five different initial concentrations of phenol (10, 20, 35, 45, and 55 mg/l) were investigated for photocatalytic performances. The pH of the solution remained at its natural pH around 6.2 for the entire experiment. The solutions were exposed to sunlight. In order to assure the similar sunlight irradiation, the works were carried out at the same time and duration for every experiment. The complete irradiation treatment usually takes about 6 h from 10 am until 4 pm. To study the effect of pH, solutions at pH 3, pH 6 (natural), and pH 12 were prepared. pH of phenol solutions was adjusted using 1 M H_2SO_4 (HmbG Chemical) and 1 M NaOH (HmbG Chemical).

2.5. Analytical procedure

The concentration of phenol was measured through UV–vis spectrophotometer (Hitachi U-2800, Japan) between the ranges of wavelength 200 to 800 nm. The maximum absorbance wavelength (λ max) for phenol is 270 nm. The degradation efficiency of phenol after photocatalytic study is shown in Eq. (1):

$$\text{Photodegradation efficiency} = \frac{C_0 - C_t}{C_0} \times 100\% \quad (1)$$

where C_t is the phenol concentration at reaction time t (h) and C_0 is the initial concentration. Chemical oxygen demand (COD) parameter was measured with HACH DR2800 spectrophotometer.

3. Result and discussion

3.1. Surface morphology

Fig. 1 presents the SEM micrographs of ZnO-P and ZnO-H. Each synthesized ZnO has its own distinguish morphology. Fig. 1(a) shows densely packed calcined ZnO-P nanoparticles, which were synthesized through precipitation method. Nanoparticles in pseudo-spherical shape could be observed. The morphology of the nanoparticles obtained was comparable to the synthesized ZnO by Chen et al. [19] who reported the morphology of nano-sized ZnO from direct precipitation was pseudo-spherical shape. A magnified image in Fig. 1(b) assists in size estimation of the ZnO-P

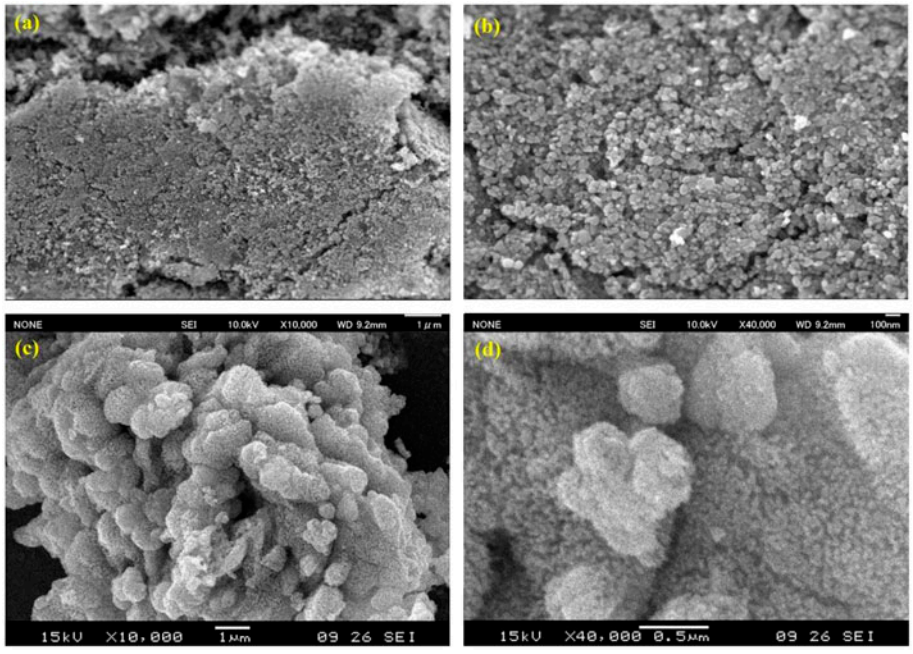

Fig. 1. SEM micrograph for synthesized ZnO-P and ZnO-H. (a) ZnO-P (×10,000), (b) ZnO-P (×40,000), (c) ZnO-H (×10,000), and (d) ZnO-H (×40,000).

nanoparticles. It is apparent that the approximate particle sizes for ZnO-P are 20–130 nm. Several studies have estimated the particle sizes of ZnO, but the sizes are varied. Lanje et al. [20] obtained 40 nm uniform spherical ZnO synthesized through precipitation of zinc nitrate and sodium hydroxide starch. However, larger particles size (3,500 ± 280 nm) formed through alkaline precipitation of zinc nitrate and triethanolamine [21]. The difference in particles size can be explained by the fact that the size of the particles could be dependent on the stabilizing agent used during precipitation process.

Meanwhile, Fig. 1(c) and (d) show the calcined ZnO-H under hydrothermal condition composed of agglomeration of ZnO-H particles. The average agglomerate size was around 71 nm. The agglomeration formed severely due to the reaction rate for the formation of ZnO increases at higher temperature [21]. Thus, it leads to the formation of larger particle and agglomeration of ZnO [22]. This agglomeration tends to reduce the photocatalytic activity of ZnO-H due to the lower surface area for the reaction to occur. Elamin and Elsanousi [23] suggested the nanoparticles aggregation which assembles in one-dimensional order cause the growth of ZnO nanosheets through hydrothermal method.

However, all of the particles are uniform pseudo-spherically shaped. Besides, the particle sizes of ZnO-H are in the same range with ZnO-P which is 20–130 nm. The similar shape with ZnO-P was obtained due to the same chemical composition used for this synthesis process. The particles size of ZnO obtained from hydrothermal synthesis is large due to the high temperature and autogenous pressure during hydrothermal process. The increase in temperature during growth and sintering causes the increase in particle size [24]. Pal et al. [25] reported the agglomeration and larger size of the ZnO nanostructures synthesized through hydrothermal method.

3.2. Crystallite phase

It is important to note that a particle consists of a group of elementary particles. The elementary particles itself is usually referred to crystallite [21]. Thus, the relationship between particle size and crystallite is important in this study.

The crystal structure and the physical state of the photocatalyst can be interpreted from the positions, intensities, and shape of the XRD peaks. The XRD patterns were used to analyze details of the ZnO structures. Fig. 2 represents the XRD patterns of all synthesized ZnO photocatalysts.

There are nine diffraction peaks observed between 20˚ and 80˚. Particularly, the strongest characteristic peaks were observed at 2θ of 36.24˚ and 36.31˚, respectively, for ZnO-P and ZnO-H which corresponds to plane (1 0 1). The (1 0 1) plane has the highest relative intensity (100%) for the entire XRD pattern evaluated compared to the other diffraction peak. Based on the phase identification analysis, all synthesized ZnO indicates the same crystallographic parameters. The peak indexed as hexagonal with space group P 63 m c (186) with a lattice constant of a = 3.25 Å and c = 5.21 Å.

However, there are differences in the intensity ratios among peaks. The intensity of each peak is caused by the crystallographic structure of the particles. The synthesized ZnO-H shows sharper diffraction peaks compared to the synthesized ZnO-P. A possible explanation for this might be due to the increase in the crystallite size [26]. As can be seen from Fig. 2, the lowest peak has the broader bottom. This is another indicator for the smaller crystallite size [27].

The XRD pattern obtained also shows no significant diffraction peak which related to the impurities. This verified the purity of the synthesized ZnO obtained in this study. The result is supported by Chen et al. [19] who obtained the same diffraction peak of XRD for the synthesized nano-sized ZnO powder yielded through precipitation method. The XRD results verified that the synthesis method applied in this study was effective in producing pure ZnO photocatalyst. This is because the synthesized ZnO was identified as zinc oxide for ZnO-P and ZnO-H during the search match database analysis. The results of this study interestingly indicate all the characteristic peaks observed in synthesized ZnO are in a good agreement with the standard data of ZnO standard taken from the Joint Committee of Powder Diffraction Standard card No. 36-1451 [28]. Details of the

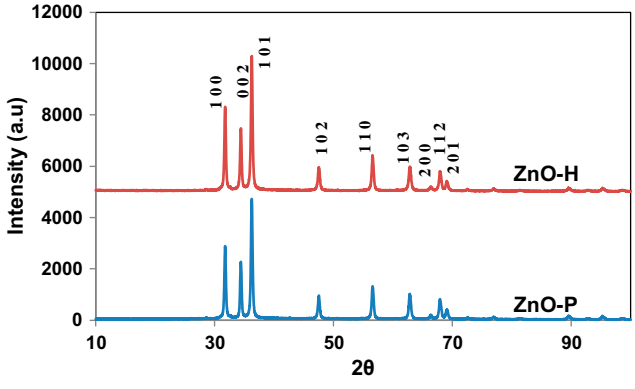

Fig. 2. XRD pattern of synthesized ZnO-P and ZnO-H.

Table 1
Comparison of standard XRD data of ZnO with measurement from XRD analysis data of synthesized ZnO

			ZnO-P		ZnO-H	
hkl	Standard 2θ (°)	Standard intensity	2θ (°)	Intensity	2θ (°)	Intensity
1 0 0	31.769	57,000	31.8	2,900	31.8	3,300
0 0 2	34.421	44,000	34.44	2,290	34.43	2,500
1 0 1	36.252	100,000	36.24	4,710	36.31	5,300
1 0 2	47.538	23,000	47.56	850	47.58	950
1 1 0	56.602	32,000	56.60	1,350	56.59	1,400
1 0 3	62.862	29,000	62.82	1,050	62.90	1,000
2 0 0	66.378	04,000	66.40	200	66.40	200
1 1 2	67.961	23,000	67.97	800	67.90	800
2 0 1	69.100	11,000	69.13	400	69.20	400

comparison between the ZnO standard pattern and synthesized pattern are shown in Table 1.

The broader diffraction peak and its intensity are varied for all three photocatalysts. Based on these two data, the crystallite size of the ZnO photocatalysts can be estimated. Narrower and higher peak of the diffraction indicates a large crystallite size. The mean crystallite sizes of ZnO were calculated using Debye Scherrer equation as shown in Eq. (2) [28]:

$$D = \frac{k\lambda}{\beta \cos\theta} \tag{2}$$

where k is a Scherrer constant = 0.9, λ is X-ray wavelength, β broadening of diffraction peak at its half maximum intensity (FWHM), and θ is Bragg diffraction angle. However, the application of Scherrer equation is only limited to nanoscales particles. Mostly, it is not applicable to grain larger than 0.1 μm [29,30]. In this study, all synthesized ZnO photocatalysts are in the form of nanoparticles.

Table 2 shows the calculated crystallite size for ZnO-P and ZnO-H. From the result, the crystallite sizes for ZnO-P and ZnO-H are almost similar. This may due to the same chemical composition during the synthesis process. ZnO-H has slightly larger crystallite size compare to ZnO. This may be due to the sufficient thermal energy that supplies to the ZnO-H during the synthesis process [28]. Moreover, the crystallite size for ZnO-P and ZnO-H is almost the same with the lowest range of the particle size (±20 nm). Theoretically, one particle is considered as single crystallite particle when the crystallite size is the same with particle sizes [21]. Thus, it can be said that some of the ZnO-P and ZnO-H considered as single crystallite particles.

Table 2
Crystallite size for synthesized ZnO-P and ZnO-H

Synthesized photocatalyst	Crystallite size (nm)
ZnO-P	23.09
ZnO-H	24.70

3.3. Nitrogen adsorption–desorption isotherm

Fig. 3 represents the result for the nitrogen adsorption–desorption isotherm of ZnO-P and ZnO-H with a general type IV. While, the hysteresis loop resembled to type IV could be observed between 0.9 and 1.0 which indicate both ZnO-P and ZnO-H have definite mesoporous structure.

The pore size distribution of ZnO-P depicts a maximum at 2.00 nm and 1.80 for ZnO-H based on the BJH analysis shown in Fig. 4. This indicates that the major pore size for ZnO-P and ZnO-H was 2.00 and 1.80 nm, respectively, and the rest are above the majority size. This result correlated with the nitrogen adsorption–desorption isotherm result which indicates that the ZnO-P obtained is a mesoporous material. While, for ZnO-H obtained, there is mix of micropores and mesopores. Thus, this condition explained the relatively low degradation rate of ZnO-H compared to ZnO-P. Finally, as a comparison, the BET surface area for ZnO-P is 11.00 and 14.60 m^2/g for ZnO-H. Both catalysts obtained almost similar surface area and characterized as a low porosity material.

3.4. Photocatalytic study

3.4.1. Effect of sunlight

In order to distinguish between the photocatalytic and adsorption reaction that might occur during the

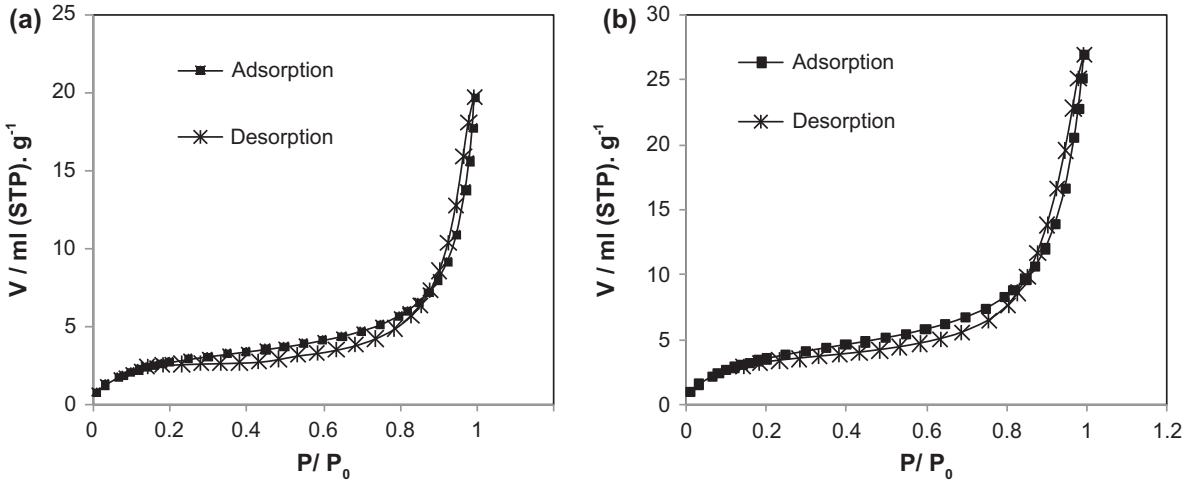

Fig. 3. Nitrogen adsorption–desorption isotherm of (a) ZnO-P and (b) ZnO-H.

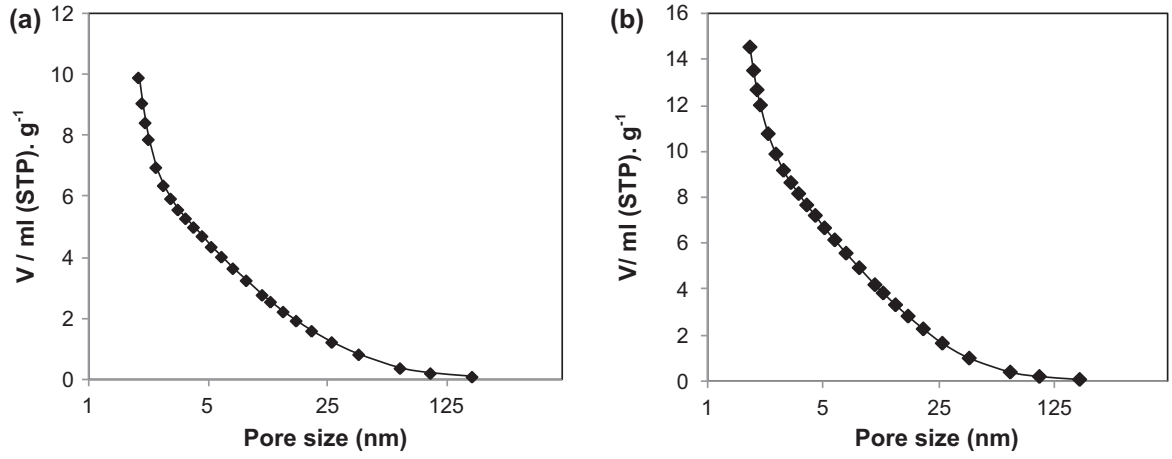

Fig. 4. BJH pore size distribution (a) ZnO-P and (b) ZnO-H.

treatment process, the experiment was conducted under dark condition for comparison with the study under sunlight irradiation. The result is shown in Fig. 5. The removal efficiency of phenol without sunlight was recorded as 2.4 and 5% for ZnO-P and ZnO-H, respectively. Removal of phenol might be due to the adsorption. Compared to the removal efficiency under sunlight irradiation, the phenol degradation recorded was above 80% for both ZnO-P and ZnO-H. This result revealed that the major reaction occurred in this treatment process is photocatalytic degradation where the reaction initiated by the radiation energy that causes the movement of electron and creates electron/hole to produce hydroxyl radical for degradation of phenol molecules.

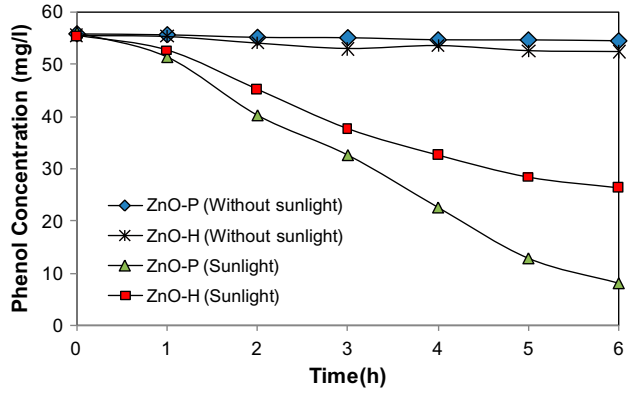

Fig. 5. Photocatalytic degradation of phenol with and without sunlight.

3.4.2. Effect of initial concentration

In order to assess the photocatalytic degradation ability of ZnO-P, and ZnO-H, different initial concentrations of phenol were studied with suspension of the synthesized ZnO. The degradation of phenol within 6 h of irradiation yielded different results based on the initial concentration. Figs. 6(a) and 7(a) present the intercorrelation among five different initial concentrations of phenol with each type of synthesized ZnO.

Fig. 6(b) represents the photodegradation of phenol for photocatalyst of ZnO-P. It is apparent that the fastest degradation was recorded at 10 mg/l of phenol. The phenol molecules were degraded 77.7% after 1 h of irradiation under solar light. Within half of the irradiation duration which was 3 h, 10 mg/l of phenol was totally degraded. Impressive result also achieved in concentration of 20 and 30 mg/l, where around 92.9 and 76.31% of phenol was removed, respectively. However, the degradation rates gradually reduced after 3 h of treatment. Only after 5 and 6 h, total degradation was achieved in 20 and 30 mg/l of initial phenol concentration.

This type of condition occurs due to the insufficient active sites on the ZnO-P for the photocatalytic reaction [31]. With the increasing amount of phenol molecules, the competition for the active sites was high and thus lowered the photocatalytic degradation. Besides, for 40 and 50 mg/l, the percentage removal was only 88.8 and 85.8%, respectively, at the end of the irradiation. Eventually, the phenol concentration is indirectly proportional to the degradation rate. As the concentration increases, the percentage of degradation would decrease. Parida et al. [32] studied the photocatalytic activity of ZnO prepared by various methods where they reported that the percentage of degradation in a mixture of 50 mg/l of 4-nitrophenol and 20 mg/l of chromium (VI) decreased from 100 to 40.9% as the pollutant concentration increased.

The effect of initial concentration was also studied with ZnO-H to verify its photodegradation capability. During the 3rd hour of irradiation to sunlight, only 100% degradation was achieved in 10 mg/l of phenol, 69.2% degradation for 20 mg/l, 47.8% for 30 mg/l, and 36.13 and 32.03% for 40 and 50 mg/l, respectively. Compared with photocatalytic degradation of ZnO-P, photocatalytic activity of ZnO-H was lower.

Based on Fig. 7(b), it is obvious that complete phenol degradation could be achieved until the initial phenol concentration of 20 mg/l within 6 h. However, the overall percentage removals in the other phenol concentrations are more than 50%. This result indicated that the synthesized ZnO-H was able to degrade phenol until 20 mg/l within 6 h of solar light irradiation. However, further prolonged reaction times are required for the total degradation to be achieved in higher phenol concentration.

The same hydrothermal method was used by Elamin and Elsanousi [23], to synthesized ZnO nanomaterials in the form of nanotubes and nanosheets and photodegradation of methyl orange was considered to be more than 90% with only 0.04 g of ZnO powder used. A recent study by Wirunmongkol et al. [33] reported that the photocatalytic activity of the ZnO powders prepared through hydrothermal process (60˚C for 6 h) using Thai autoclave unit is almost equal to commercial grade ZnO powder.

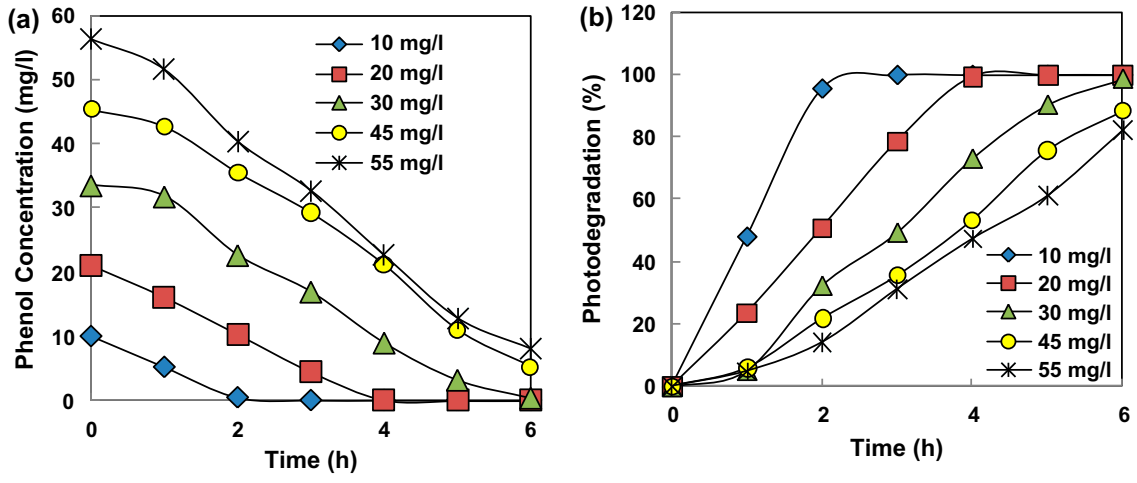

Fig. 6. (a) Photocatalytic degradation of phenol by ZnO-P with different initial concentration and (b) phenol percentage removal (ZnO-P catalyst loading = 0.6 g, initial pH 6.2).

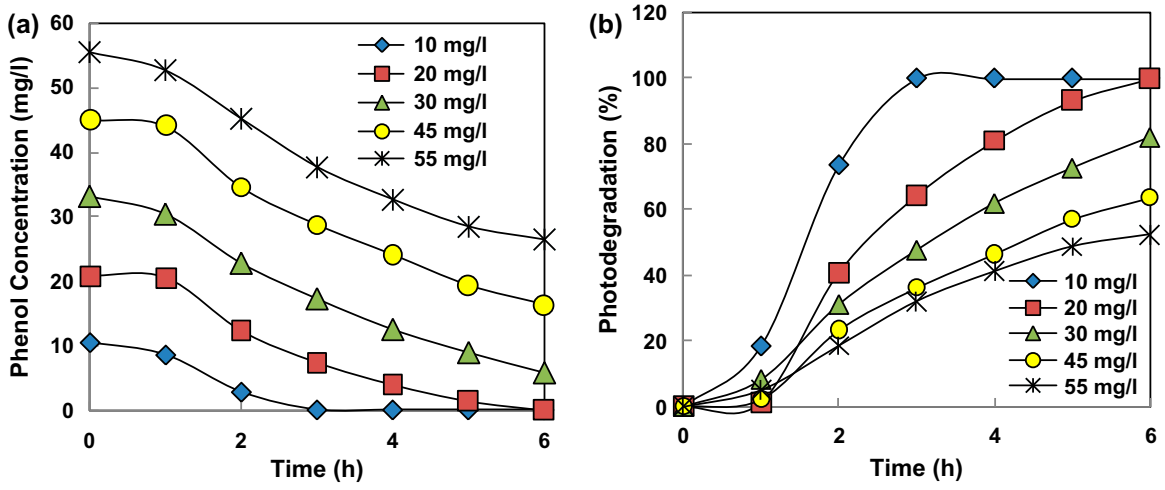

Fig. 7. (a) Photocatalytic degradation of phenol by ZnO-H with different initial concentration and (b) phenol percentage removal (ZnO-H catalyst loading = 0.6 g, initial pH 6.2).

The main focus in photocatalytic reaction is to generate $^{\bullet}OH$ and $^{\bullet}O_2^-$ on the surface of the catalyst to initiate the reaction. Several factors such as catalyst loading, light intensity, and duration of irradiation influence the amounts of the production of these two ions. These factors remain unchanged throughout the reaction period, the amount of $^{\bullet}OH$ and $^{\bullet}O_2^-$ is constant. Generally, the degradation rate of phenol decreases as the concentration increases. This is due to the inadequate $OH^{\bullet}$ radicals for the photocatalytic reaction in higher substrate concentration. In the case of the synthesized catalyst, other several factors affect the degradation of phenol. For instance, different particle sizes and the morphology of the catalyst will yield different photocatalytic degradation performances.

3.4.3. Effect of pH

The pH of the wastewater can be varied significantly and influence the degradation behavior of the organic compound such as phenol. In this study, the effect of pH was conducted in order to study the photodegradation performances in various pH conditions. For ZnO-P and ZnO-H photocatalysts, the photodegradation performances were studied under pH 3, natural (pH 6), and pH 12. Based on Fig. 8(a) and (c), the total degradation of phenol was recorded in pH 3 and pH (natural) for both type of synthesized ZnO. Three hours are needed for phenol molecules to be fully degraded by ZnO-P and ZnO-H. Thus, the performances rate can be compared during the 2 h of irradiation.

For ZnO-P photocatalyst, total of 94.8% of phenol molecules was degraded in acidic (pH 3) condition, while 83.0% in natural condition (pH 6). This result is presented in Fig. 8(b). Similar results were observed ZnO-H photocatalyst in Fig. 8(d). In natural pH, the degradation was 81.2%. Interestingly, acidic condition is favorable for ZnO-H where 99.5% of phenol was degraded in 2 h of irradiation. Singh et al. [34] suggested that pH is an important parameter in the heterogeneous photocatalysis reaction because it influences the adsorption behavior of the pollutant on the aggregates size that formed and most importantly the surface charge of the photocatalyst. Besides, pH of the solution will also affect the electrostatic interaction between semiconductor surface, solvent molecules, substrate, and charged radical during photocatalytic reaction [35]. Moreover, the occurring of the protonation and deprotonation of phenol also affected the pH of the solution [36]. The properties profoundly affected by the solution pH were surface charge and ionization or speciation (pKa) of phenol. Initially, pKa value of phenol is 9.95. At pH below phenol pKa value, the organic compound exists as neutral species. While, when pH solution was above pKa value, phenol molecules attain a negative charge.

In Fig. 8(b) and (d), there is a significant trend which shows the decrease of photodegradation as the pH increases. In alkaline condition, the percentage of degradation recorded was 54.5 and 60.9% for ZnO-P and ZnO-H, respectively. This could be due to the pKa value of phenol is 9.95 and point of zero charge (P_{ZC}) of ZnO is 9.0, both are negatively charged in pH 12. This is because pH of the solution is higher than pKa value and P_{ZC}. Since both are in negative charge, phenol molecules repelled away from ZnO surface and lowered the photodegradation. Pardeshi and

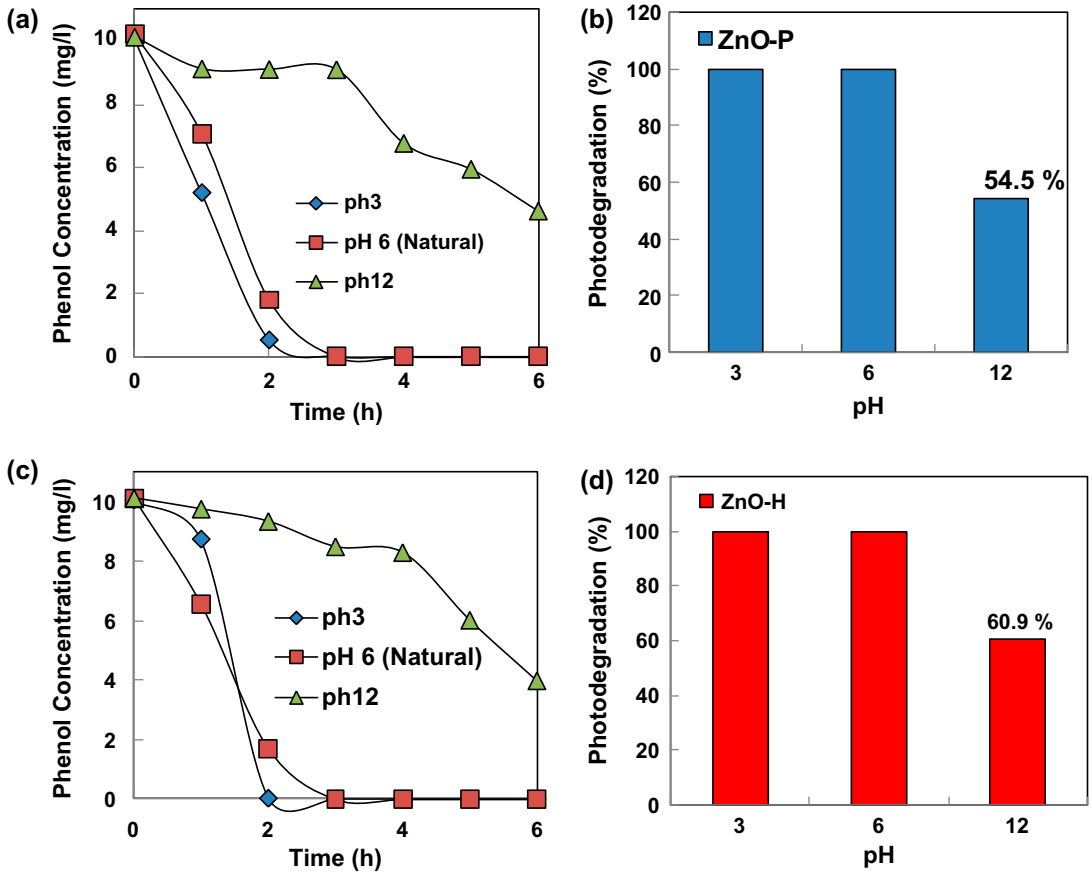

Fig. 8. Photocatalytic degradation of phenol in different pH (a) degradation of phenol by ZnO-P (b) photodegradation percentage of ZnO-P (c) degradation of phenol by ZnO-H and (d) photodegradation percentage of ZnO-H (phenol initial concentration = 10 mg/l, catalyst loading = 0.6 g).

Patil [37] performed similar experiments through zinc oxide suspension in aqueous solution of phenol under irradiation of solar energy. The optimum pH for phenol degradation was pH 5–7 [37]. While, for ZnO prepared by various methods by Parida and Parija [12], the optimum pH for degradation of 4-nitrophenol was pH 6.

3.4.4. Kinetics study

Generally, the photocatalytic reactions mechanism consists of two steps. The first step is fast adsorption of the reactants on the catalyst surface and a slow step of reaction in the adsorbed phase of the organic compound. Then, it is followed by the photogenerated hydroxyl radical [24]. The kinetics of photocatalytic reactions of phenol could be described in the Langmuir–Hinshelwood model. The efficiency of different photocatalysts on the photocatalytic rate was investigated. Fig. 9 depicts the plot graph of ln C_0/C as a function of time for photodegradation of phenol which follows a pseudo-first-order kinetics behavior.

Table 3 shows the apparent rate constant (k) obtained from the plotted graph, which is 1.1305 and

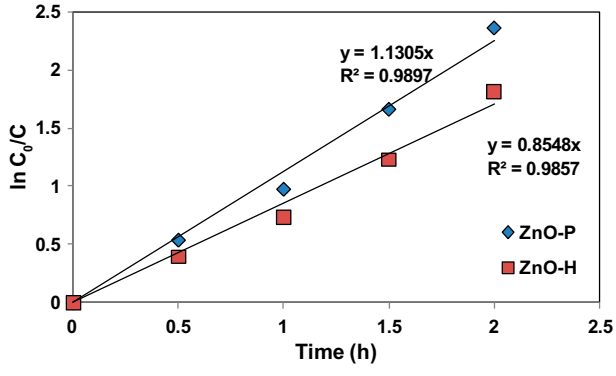

Fig. 9. Plot of C_0/C against time (h) for ZnO-P and ZnO-H.

0.8548 h^{-1} for photocatalysts ZnO-P and ZnO-H, respectively. The apparent rate constant is proportional to the efficiency of the photocatalysts. The higher efficiency shows a higher k value. This result shows the relationship between the rates of surface catalyst reactions to the surface covered by substrate. A higher degradation rate indicates more hydroxyl groups and water molecules at the surface of the photocatalyst thus promote the degradation of phenol [38].

Many researchers observed the reduction rate in photocatalytic reaction of organic compound through Langmuir–Hinshelwood model. Han et al. [39] intensively evaluated the photocatalytic of estrone by ZnO under artificial UVA irradiation using Langmuir–Hinshelwood model for every parameters studied. All results obtained are well fitted with the kinetic model. Besides, the kinetics of photooxidation of organic water impurities on illuminated titanium dioxide is based on a Langmuir–Hinshelwood model [40]. The reaction regarded as first-order behavior with the correlation factor R^2 = 0.94. The photocatalytic degradation of phenol by solgel-synthesized ZnO by Banhebal et al. [41] was described as first-order kinetic model.

3.5. Mineralization of phenol

The mineralization of phenol was monitored through the reduction of COD in phenol solution after 12 h of reaction time. Based on Fig. 10, it clearly shows that the reduction trends are unstable. The COD value was increased within the reaction time and then continues to decrease back at certain reaction time. However, obvious reduction of COD was monitored during the first hour of reaction. This might be due to the rapid degradation of phenol molecules after being contacted with ZnO. Another crucial reaction happened during the fourth hour of reaction. The COD value for both synthesized ZnO was increased and slowly decreased until the last twelfth hour. The percentage of COD removal at the end of the experiment for ZnO-P and ZnO-H was 87.7 and 71.4%, respectively.

Table 3
Pseudo-first-order apparent constant values for different synthesized ZnO-P and ZnO-H (catalyst loading = 0.6 g, initial pH 6.2)

C_0 (mg/l)	K (h^{-1})	R^2
ZnO-P	1.1305	0.9897
ZnO-H	0.8548	0.9857

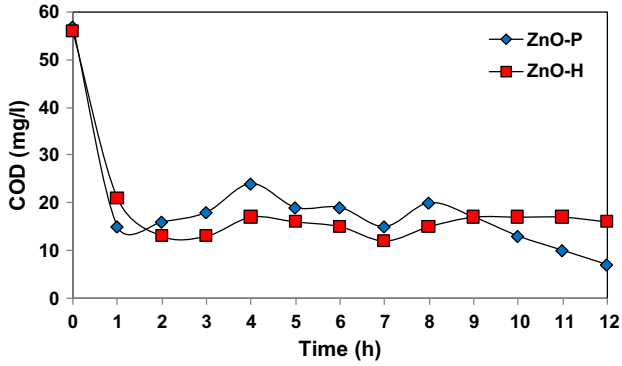

Fig. 10. COD monitoring in photocatalytic degradation of phenol by ZnO-P, ZnO-H (ZnO catalyst loading = 0.6 g, initial pH 6.2).

The remaining chemicals in phenol solution are not totally mineralized which could be due to intermediate that formed as by-products during mineralization [42]. Although the total degradation of phenol molecules under the solar irradiation can be achieved easily after 6 h, this could not guarantee the total mineralization of phenol. The reaction time needed to be prolonged until producing only carbon dioxide and water as the end product. However, Pardeshi and Patil [37] verified in their studies that the mineralization of phenol under sunlight is faster than the xenon lamp irradiation. It takes 8 h for 75 mg/l of phenol to mineralize under sunlight irradiation but more than 9 h for xenon lamp irradiation. Ba-Abbad et al. [43] gained a remarkable result, where the COD was reduced to 96% only within 1 h of radiation using ZnO. The reduction of COD value correlated to the degradation of the pollutant. Under UV irradiation, photocatalytic reactions with semiconductor materials involve the generations and separation electron-hole pairs [44] and consequently degraded the pollutant.

4. Conclusion

ZnO photocatalyst was successfully synthesized through precipitation (ZnO-P) and hydrothermal (ZnO-H) methods. The particles shape formed is in pseudo-spherical shape with the range size within 20–130 nm. Some obvious agglomerates were formed in ZnO-H with the agglomerates size 71 nm. The XRD patterns of synthesized ZnO are in pure phase as no characteristic peaks were observed for other impurities, and the crystallite size obtained is 23.09 nm and 24.7 nm. ZnO-P was capable to achieve total degradation of phenol until 30 mg/l of initial phenol concentration, while for ZnO-H, the highest concentration of phenol removal was 20 mg/l. The fastest degradation

was under acidic condition (pH 3) and followed by natural condition. In alkaline condition, the percentage of degradation recorded was 54.5 and 60.9% for ZnO-P and ZnO-H, respectively. The solar-photocatalytic study followed the Langmuir–Hinshelwood kinetic model. The COD monitoring verified the mineralization of phenol after 12 h only removed as much as 87.7 and 71.4% for ZnO-P and ZnO-H, respectively.

References

[1] T. Damstra, J. Pronczuk, Persistent Organic Pollutants (POPs). Children Health and Environment (2008). Available from: <http://www.who.int/ceh/capacity/POPs.pdf>.

[2] L. Yang, Z. Li, L. Zou, H. Gao, Removal capacity and pathways of phenolic endocrine disruptors in an estuarine wetland of natural reed bed, Chemosphere 83(3) (2011) 233–239.

[3] S. Chaliha, K.G. Bhattacharyya, Catalytic wet oxidation of phenol and its derivatives with Fe_2O_3 and MnO_2, Ind. J. Chem. Technol. 13 (2006) 499–504.

[4] R. McKinlay, J.A. Plant, J.N.B. Bell, N. Voulvoulis, Endocrine disrupting pesticides: Implications for risk assessment, Environ. Int. 34(2) (2008) 168–183.

[5] S.A. Snyder, S. Adham, A.M. Redding, F.S. Cannon, J. DeCarolis, J. Oppenheimer, Role of membranes and activated carbon in the removal of endocrine disruptors and pharmaceuticals, Desalination 202(1–3) (2007) 156–181.

[6] M. Auriol, Y. Filali-Meknassi, R.D. Tyagi, C.D. Adams, R.Y. Surampalli, Endocrine disrupting compounds removal from wastewater, a new challenge, Process Biochem. 41(3) (2006) 525–539.

[7] D. Chen, A.K. Jay, Photocatalytic kinetics of phenol and its derivatives over UV irradiated TiO_2, Appl. Catal. B 23(2–3) (1999) 143–157.

[8] A. Fujishima, T.N. Rao, D.A. Tryk, Titanium dioxide photocatalysis, J. Photochem. Photobiol. C 1(1) (2000) 1–21.

[9] R.M. Abhang, D. Kumar, S.V. Taralkar, Design of photocatalytic reactor for degradation of phenol in wastewater, Int. J. Chem. Eng. Appl. 2(5) (2011) 337–341.

[10] A. Khani, M.R. Sohrabi, Simultaneous synthesis-immobilization of nano ZnO on perlite for photocatalytuc degradation of an azo dye in semi batch packed bed photo-reactor, Pol. J. Chem. Technol. 14 (2012) 69–76.

[11] M.Y. Ge, H.P. Wu, L. Niu, J.F. Liu, S.Y. Chen, P.Y. Shen, Nanostructured ZnO: From monodisperse nanoparticles to nanorods, J. Cryst. Growth 305(1) (2007) 162–166.

[12] K.M. Parida, S. Parija, Photocatalytic degradation of phenol under solar radiation using microwave irradiated zinc oxide, Sol. Energy 80(8) (2006) 1048–1054.

[13] N. Daneshvar, M.H. Rasoulifard, A.R. Khataee, F. Hosseinzadeh, Removal of C.I. Acid Orange from aqueous solution by UV irradiation in the presence of ZnO nanopowder, J. Hazard. Mater. 143(1–2) (2006) 95–101.

[14] E.N.S. Muccillo, S.K. Tadokoro, R. Muccillo, Physical characteristics and sintering behavior of MgO-doped ZrO_2 nanoparticles, J. Nanopart. Res. 6(2/3) (2004) 301–305.

[15] L. D'souza, R. Richards, Synthesis of metal-oxide nanoparticles: Liquid–solid transformation, in: A. Rodriquez, M. Fernández-García (Ed.), Synthesis, Properties, and Application of Oxide Nanomaterials, Wiley, Hoboken, NJ, 2007, pp. 81–117.

[16] T. Sahoo, M. Kim, J.H. Baek, S.R. Jeon, J.S. Kim, Y.T. Yu, C.R. Lee, I.H. Lee, Synthesis and characterization of porous ZnO nanoparticles by hydrothermal treatment of as pure aqueous precursor, Mater. Res. Bull. 46(4) (2011) 525–530.

[17] S. Zandi, P. Kameli, H. Salamati, H. Ahmadvand, M. Hakimi, Microstructure and optical properties of ZnO nanoparticles prepared by a simple method, Physica B 406(17) (2011) 3215–3218.

[18] M. Rezapour, N. Talebian, Comparison of structural, optical properties and photocatalytic activity of ZnO with different morphologies: Effect of synthesis methods and reaction media, Mater. Chem. Phys. 129(1–2) (2011) 249–255.

[19] C. Chen, P. Liu, C. Lu, Synthesis and characterization of nano-sized ZnO powders by direct precipitation method, J. Chem. Eng. 144(3) (2008) 509–513.

[20] A.S. Lanje, S.J. Sharma, R.S. Ningthoujam, J.S. Ahn, R.B. Pode, Low temperature dielectric studies of zinc oxide (ZnO) nanoparticles prepared by precipitation method, Adv. Powder Technol. 24 (2013) 331–335.

[21] D. Li, H. Haneda, Morphologies of zinc oxide particles and their effects on photocatalysis, Chemosphere 51(2) (2003) 129–137.

[22] Z.H. Liu, Y. Kanjo, S. Mizutani, Removal mechanisms for endocrine disrupting compounds (EDCs) in wastewater treatment-physical means, biodegradation, and chemical advanced oxidation: A review, Sci. Total Environ. 407(2) (2009) 731–748.

[23] N. Elamin, A. Elsanousi, Synthesis of ZnO nanostructures and their photocatalytic activity, J. Appl. Ind. Sci. 1 (2013) 32–35.

[24] K. Hayat, M.A. Gondal, M.M. Khaled, S. Ahmed, A.M. Shemsi, Nano ZnO synthesis by modified sol gel method and its application in heterogeneous photocatalytic removal of phenol from water, Appl. Catal A 393(1–2) (2011) 122–129.

[25] U. Pal, J.G. Serrano, P. Santiago, G. Xiong, K.B. Ucer, R.T. Williams, Synthesis and optical properties of ZnO nanostructures with different morphologies, Opt. Mater. 29(1) (2006) 65–69.

[26] M. Ristić, S. Musić, M. Ivanda, S. Popović, Sol–gel synthesis and characterization of nanocrystalline ZnO powders, J. Alloys Compd. 397(1–2) (2005) L1–L4.

[27] Y. Abdollahi, A.H. Abdullah, Z. Zainal, N.A. Yusof, Synthesis and characterization of manganese doped ZnO nanoparticles, Int. J. Basic Appl. Sci. 11 (2011) 62–69.

[28] D. Raoufi, Synthesis and microstructural properties of ZnO nanoparticles prepared by precipitation method, Renewable Energy 50 (2013) 932–937.

[29] A. Obadiah, R. Kannan, P. Ravichandran, A. Ramasubbu, K. Vasanth, Nano hydrotalcite as a novel catalyst for biodiesel conversion, Dig. J. Nanomater. Biostruct. 1(7) (2012) 321–327.

[30] N.F. Atta, A. Galal, S.M. Ali, The catalytic activity of Ruthenates ARuO3 (A=Ca, Sr or Ba) for hydroegen evaluation reaction in acidic medium, Int. J. Electrochem. Sci. 7 (2012) 725–746.
[31] M. Zulfakar, N.A.H. Hairul, H.M.R. Akmal, M.A. Rahman, Photocatalytic degradation of phenol in a fluidized bed reactor utilizing immobilized TiO_2 photocatalyst: Characterization and process studies, J. Appl. Sci. 11(13) (2011) 2320–2326
[32] K.M. Parida, S.S. Dash, D.P. Das, Physico-chemical characterization and photocatalytic activity of zinc oxide prepared by various methods, J. Colloid Interface Sci. 298(2) (2006) 787–793.
[33] T. Wirunmongkol, N. O-Charoen, S. Pavasupree, Simple hydrothermal preparation of zinc oxide powders using Thai autoclave unit, Energy Pro. 34 (2013) 801–807.
[34] H.K. Singh, M. Saquib, M.M. Haque, M. Muneer, D.W. Bahnemann, Titanium dioxide mediated photocatalysed degradation of phenoxyacetic acid and 2,4,5-trichlorophenoxyacetic acid, in aqueous suspensions, J. Mol. Catal. A: Chem. 264(1–2) (2007) 66–72.
[35] S. Ahmed, M.G. Rasul, W.N. Martens, R. Brown, M.A. Hashib, Heterogeneous photocatalytic degradation of phenols in wastewater: A review on current status and developments, Desalination 261(1–2) (2010) 3–18.
[36] P.R. Shukla, S. Wang, H.M. Ang, M.O. Tadé, Photocatalytic oxidation of phenolic compounds using zinc oxide and sulphate radicals under artificial solar light, Sep. Purif. Technol. 70(3) (2010) 338–344.
[37] S.K. Pardeshi, A.B. Patil, A simple route for photocatalytic degradation of phenol in aqueous zinc oxide suspension using solar energy, Sol. Energy 82(8) (2008) 700–705.
[38] A. Idris, N. Hassan, R. Rashid, A.F. Ngomsik, Kinetics and regeneration studies of photocatalytic magnetic seperable beads for chromium (VI) reduction under sunlight, J. Hazard. Mater. 186(1) (2010) 629–635.
[39] J. Han, Y. Liu, N. Singhal, L. Wang, W. Gao, Comparative photocatalytic degradation of estrone in water by ZnO and TiO_2 under artificial UVA and solar irradiation, J. Chem. Eng. 213 (2012) 150–162.
[40] A. Sobczyński, Ł. Duczmal, W. Zmudziński, Phenol destruction by photocatalysis on TiO_2: An attempt to solve the reaction mechanism, J. Mol. Catal. A: Chem. 213(2) (2004) 225–230.
[41] H. Benhebal, M. Chaib, T. Salmon, J. Geens, A. Leonard, S.D. Lambert, M. Crine, B. Heinrichs, Photocatalytic degradation of phenol and benzoic acid using zinc oxide powders prepared by the sol–gel process, Alexandria Eng. J. 52 (2013) 517–523.
[42] E. Grabowska, J. Reszczyńska, A. Zaleska, Mechanism of phenol photodegradation in the presence of pure and modified-TiO_2: A review, Water Res. 46(17) (2012) 5453–5471.
[43] M.M. Ba-Abbad, A.A.H. Kadhum, A.B. Mohamad, M.S. Takriff, K. Sopian, Solar photocatalytic degradation of environmental pollutants using ZnO prepared by sol–gel: 2, 4-dichlorophenol as case study, Int. J. Therm. Environ. Eng. 1(1) (2010) 37–42.
[44] F. Lin, B. Cojocaru, C.L. Chou, C.A. Cadigan, Y. Ji, D. Nordlund, T.C. Weng, Z. Zheng, V.I. Pârvulescu, R.M. Richards, Photocatalytic activity and selectivity of ZnO materials in the decomposition of organic compounds, ChemCatChem. 5(12) (2013) 3841–3846.